Eur. Phys. J. Special Topics **226**, 2843–2851 (2017)

DOI: 10.1140/epjst/e2016-60371-8

THE EUROPEAN PHYSICAL JOURNAL SPECIAL TOPICS

Regular Article

Controlling correlated particles and generating entanglement in an ac-driving lattice

Yi Zheng, Shi-Jie Yang[a]

Department of Physics, Beijing Normal University, Beijing 100875, P.R. China

Received 23 November 2016 / Received in final form 24 January 2017
Published online 26 July 2017

Abstract. The quantum tunneling of correlated atoms in an optical lattice is investigated in the presence of ac-driving fields. The effective Hamiltonian with density-dependent hopping rates are deduced. The migration of a correlated atoms in 1D and 2D lattices can be realized. Based on this mechanism, we propose a method to create two-partite entanglement. Our model may provide applications in quantum computing and quantum information in ultracold atoms.

1 Introduction

Quantum simulation is a potential area for exploring fundamental many-body physics. Ultracold quantum gases in optical lattices have become one of the most powerful quantum simulators due to the high level of controllability and cleanness [1,2]. The lattice system prevails since the experimental techniques has enabled single-site resolved detection with high fidelity [3–5]. Thus paradigm models, such as the tight-binding Hubbard models [6–9], the Harper Hamiltonians with artificial gauge fields [10,11], are now achievable. At the same time, significant phenomena were demonstrated, ranging from the basic superfluid-Mott insulator (SF-MI) transition [7], to the (fractional) quantum Hall effects [12–15].

The accurate controllability of the parameters in lattice system leads to the investigation of many-body coherent dynamics [16,17]. With static quantum control like a potential gradient, a wave packet in the lattice undergoes the Bloch oscillations (BOs) [18]. Whereas a periodically driving problem can often be described with the aid of Floquet theory, resulting in an effective time-independent Hamiltonian [19]. Novel phenomena such as photon-assisted tunneling [20], dynamical localization (DL) [21,22], (selective) coherent destruction of tunneling (CDT) [23–27], and others [28–30], were also revealed in various driving systems. These results provide a better understanding of the solid state physics and pave the way to the exploration of the Floquet engineering [31,32]. Tunneling controls of single particle were proposed in refernce [33], where the directed CDT were realized through bipartite super-lattices and periodic driving. For strongly correlated systems, researches are focused on specific regimes like the coherent transport [34,35] and correlated BOs [36,37].

We have previously showed possible schemes of migrating correlated particle pair [38,39], where the directed CDT stems from breaking the mirror-symmetry

[a] e-mail: yangshijie@tsinghua.org.cn

of tunneling. In a 1D optical lattice, the lattice shaking combined with a periodic modulation of the on-site interaction, i.e., a double modulation (DM), is considered to generate an unconventional Hubbard model [40]. Whereas for strongly correlated system, the driving resonate to the on-site interaction can lead to photon-assisted tunneling, which reveals the possibility of controlled tunneling. The other scheme is proposed in a tilted lattice with lattice shaking. An effective time-independent Hamiltonian can be deduced by re-normalizing the hopping rates. The density evolutions of the correlated pair are simulated by applying the Schrodinger equation with the original Hamiltonian. We make use of the resulting density-dependent hoppings to generate CDT and realize directed migration. Our proposals apply to both 1D and 2D systems. Beyond the bipartite problem, such modulations can generate quantum entanglement in systems with higher population.

In this paper, we propose a new scheme to generating entanglement in the optical lattices. In Section 2 we demonstrate the driving models and corresponding effective hoppings. The 1D and 2D migration schemes are presented in Section 3 and Section 4, respectively. In Section 5, we show the control schemes to generate entanglement in 3- and 4-particle system. A summary is presented in Section 6.

2 Model

Within the framework of the Bose-Hubbard model, the bosonic atoms in a 1D deep lattice with periodic modulations can be described by the Hamiltonian,

$$\hat{H} = -J\sum_j(\hat{b}_j^\dagger\hat{b}_{j+1} + \text{h.c.}) + \frac{U(t)}{2}\sum_j \hat{n}_j(\hat{n}_j - 1) + K(t)\sum_j j\cdot\hat{n}_j, \tag{1}$$

where we assume that the on-site interaction is time-dependent because of the modulation of an external magnetic field in the vicinity of a Feshbach resonance [41,42], i.e. $U(t) = U_0 + U_1\cos(\omega t)$. The shaking lattice is represented by the last term in equation (1), where $K(t) = K_0 + K_1\cos(\omega t)$ describes a dc-ac field. The two driving frequencies are assumed to be the same for convenience. All parameters in such Hamiltonian are independently tunable in experiments. To apply the Floquet analysis, $\omega \gg J$ has to be satisfied. In such condition, $K_0 = 0$ and $U_1 = 0$ with a weak interaction (small U_0) lead to the standard renormalization of the hopping rates [43]. In a resonate case with strong interaction and $U_0 = n\omega$ (with n the integer) and $U_1 = 0$, photon-assisted tunneling occurs, which is analogous to the case with $K_0 = n\omega$ and $U_1 = 0$ [20,44]. Pioneering works on two-particle behaviors have revealed the dynamics of correlated quantum walks in a uniform lattice [45] and fractional BO in a tilted lattice [36]. These feasible manipulations provide a new test bed for engineering the relevant lattice models [10,11,20,25].

We focus on the resonate conditions, thus an energy quanta ω, provided by the lattice shaking or on-site modulation, serves as the compensation to the energy cost of multi-particle on-site occupations. A general result from the Floquet theory gives an effective Hamiltonian,

$$\hat{H}_{\text{eff}} = -\sum_{\langle i,j\rangle}\hat{b}_i^\dagger J_{\text{eff}}(\hat{n}_i,\hat{n}_j)\hat{b}_j, \tag{2}$$

where the effective hopping rate J_{eff} depends on the nearest on-site occupations and the formula varies in different situations [38,39].

3 Controlled migration in 1D

For the DM model in a 1D uniform lattice, i.e., $K_0 = 0$ while $K_1 \neq 0$ and $U_1 \neq 0$, the resonate condition $U_0/\omega = m$ (with m an integer) results in an occupation-dependent hopping rate

$$J_{(n_j,n_{j+1})\leftrightarrow(n_j+1,n_{j+1}-1)} = J\mathcal{J}_\mu\left(\frac{K_1}{\omega} - \frac{U_1}{\omega}(n_j - n_{j+1} + 1)\right),$$
$$\mu = (n_j - n_{j+1} + 1)m,$$
$$J_{(n_j,n_{j+1})\leftrightarrow(n_j-1,n_{j+1}+1)} = J\mathcal{J}_\nu\left(\frac{K_1}{\omega} - \frac{U_1}{\omega}(n_j - n_{j+1} - 1)\right),$$
$$\nu = (n_j - n_{j+1} - 1)m,$$

with $\mathcal{J}_{\mu(\nu)}$ the $\mu(\nu)$-th order Bessel function of the first kind. This formula also works when $K_1 = 0$ or $U_1 = 0$ and even $m \sim 0$. DM can break the mirror symmetry of tunneling without altering the lattice symmetry. For instance, the tunneling rates of the two process:

$$|2,0\rangle_{j,j+1} \overset{A}{\leftrightarrow} |1,1\rangle_{j,j+1} \overset{B}{\leftrightarrow} |0,2\rangle_{j,j+1} \tag{3}$$

are $J_A = J\mathcal{J}_m(\frac{K_1}{\omega} - \frac{U_1}{\omega})$ and $J_B = J\mathcal{J}_m(\frac{K_1}{\omega} + \frac{U_1}{\omega})$, which are generally unequal. To realize the directed tunneling control, the mirror-symmetry breaking is necessary. Thus by setting the driving amplitude K_1 and U_1 appropriately, it is possible to achieve $J_{(1,1)\to(0,2)} = 0$ while $J_{(1,1)\leftarrow(2,0)} \neq 0$, and vice versa.

Such selective tunneling also arise in a 1D tilted lattice with lattice shaking ($U_1 = 0$ while $K_0 \neq 0$ and $K_1 \neq 0$). However, an usual resonate condition cannot localize a single particle. We consider the specific conditions $U_0, K_0 = m\omega/2$ and $\omega \gg J$. With m an odd integer, such conditions ensure the suppression of single-particle tunneling, which can be verified from the effective hopping rates:

$$J_{(n_j,n_{j+1})\leftrightarrow(n_j+1,n_{j+1}-1)} = \begin{cases} J\mathcal{J}_{n_+}(\frac{K_1}{\omega}), & n_+ \in Z; \\ 0, & \text{otherwise}, \end{cases}$$
$$J_{(n_j,n_{j+1})\leftrightarrow(n_j-1,n_{j+1}+1)} = \begin{cases} J\mathcal{J}_{n_-}(\frac{K_1}{\omega}), & n_- \in Z; \\ 0, & \text{otherwise}, \end{cases}$$
$$n_\pm = (n_j - n_{j+1} \pm 1)\frac{U_0}{\omega} - \frac{K_0}{\omega}, \tag{4}$$

where Z represents the integer set. Applying equation (4) to the two-particle system and we assume

$$U_0 - K_0 = \mu\omega, \quad U_0 + K_0 = \nu\omega, \tag{5}$$

with μ, ν integers, the effective tunneling rates in formula (3) are $J_A = J\mathcal{J}_\mu(\frac{K_1}{\omega})$ and $J_B = (-1)^\nu J\mathcal{J}_\nu(\frac{K_1}{\omega})$. Analogous to the DM case, by tuning the value of K_1, J_A and J_B can be restrained to zero independently. When $J_B = 0$, a two particle system undergoes the Rabi-like oscillation labeled by A in the formula (3) with frequency $\omega^A_{\text{osc}} = \sqrt{2}J_A$ [46]. When $J_A = 0$, the oscillation B occurs with $\omega^B_{\text{osc}} = \sqrt{2}J_B$.

The controlled migration of the particle pair is a result of allowing oscillation A and B to occur alternatively. The condition $J_B = 0$ is held for $T = \pi/2\omega^A_{\text{osc}}$ to achieve a complete tunneling process $|2,0\rangle_{j,j+1} \overset{A}{\to} |1,1\rangle_{j,j+1}$. Then the parameters are switched to set $J_A = 0$, leading to a subsequent process $|1,1\rangle_{j,j+1} \overset{B}{\to} |0,2\rangle_{j,j+1}$.

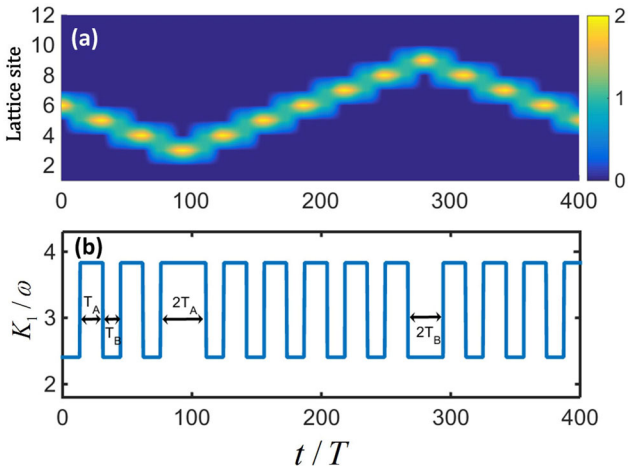

Fig. 1. (a) A realization of a zigzag pattern via combination of the leftward and rightward migration processes. The turning points are $t = 3(T_A + T_B)$ and $t = 9(T_A + T_B)$. (b) The corresponding modulation scheme of the lattice driving amplitude. $K_1/\omega = 3.8317$ in the time interval T_A and $K_1/\omega = 2.4048$ in the time interval T_B. The time is in the unit of $T = 2\pi/\omega$.

Thus the correlated pair on site j migrate to site $j + 1$, which fulfill a complete cycle. The direction of migration by the two-step manipulation depends on the preliminary occupation condition and the choice of the initial tunneling process.

To show the controllability of two-particle migration, we simulate the dynamical evolution of a bipartite system from the full time-dependent Hamiltonian equation (1). The tilted shaking lattice scheme is adopted in the present paper, which comes at a similar result from the DM scheme [38]. The relevant parameters are taken as $U_0 = K_0 = \omega/2 = 20$ (in the unit of J). Starting from a doublon state $|2, 0\rangle_{j,j+1}$ ($j = 6$), we set $K_1/\omega = K_1^B/\omega = 2.4048$ in the time interval $T_B = \pi/2\omega_{\rm osc}^B$ to meet the condition $J_A = 0$. K_1 is then switched to $K_1/\omega = K_1^A/\omega = 3.8317$ to ensure $J_B = 0$ in the time interval $T_A = \pi/2\omega_{\rm osc}^A$. Repeating the two processes gives rise to a leftward migration of the correlated pair. We label the above controlling process as $T_B - T_A$ mode, thus a rightward motion can be simply realized through a T_A-T_B mode. As shown in Figure 1a, a forth and back motion is achieved by alternatively switching from $T_B - T_A$ to $T_A - T_B$ mode at $t = 3(T_A + T_B)$ and vice visa at $t = 9(T_A + T_B)$. The corresponding modulation scheme of the amplitude K_1 is shown in Figure 1b.

The periodically driving Hubbard model in our consideration is within experimental realization with cold atoms in optical lattices [20,47,48]. With ultracold rubidium atoms, the relevant parameters, such as the tunneling rate J, the on-site interaction U and the lattice tilting K_0, can be tuned to $J/\hbar \sim 1$kHz, $J/U \sim 0.2$ and $K_0 \sim n\omega$ [20,47]. The controlling parameter K_1 can be tuned up to $4\hbar\omega$ [48]. To fit the high-frequency limit, we will consider the driving frequency to be $\omega \sim 40$ kHz. All parameters are highly controllable and can vary in a wide range, making it possible to reach the conditions in our concern.

4 Controlled migration in 2D

The researches on 2D quantum control have been stimulated by the rapid progresses of the site-resolved probing techniques [49] and 2D simulations in quantum computing [50,51]. The present particle pair quantum control through the modulated driving

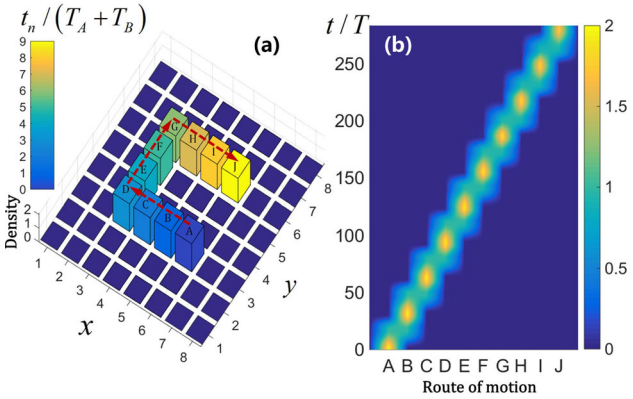

Fig. 2. 2D migration of the correlated pair on a 8×8 lattice. (a) The density peaks at discrete times $t_n = n \cdot (T_A + T_B)$, $n = 0, 1, 2, \cdots$, with n labeled by colors. The route of motion is guided by the arrows, along which the sites are labeled by "$A, B, \cdots, J$". (b) The density evolution along the anticipated route shown in (a).

scheme in a tilted lattice can be naturally extended to the 2D case. While implementing the controlling scheme in the tunneling direction (TD), we need to suppress all possible tunnelings in the direction perpendicular to the TD. All possible tunneling channels in the latter direction include $|2,0\rangle_{\langle i,j\rangle} \to |1,1\rangle_{\langle i,j\rangle}$, $|0,2\rangle_{\langle i,j\rangle} \to |1,1\rangle_{\langle i,j\rangle}$ and $|1,0\rangle_{\langle i,j\rangle} \leftrightarrow |0,1\rangle_{\langle i,j\rangle}$, where $\langle i,j\rangle$ indicate the nearest neighboring sites i, j. Referring to the 1D effective hopping rates shown in equation (2) and equation. (4), we propose the suppression scheme in the damping direction (DD) as $U/\omega^{(\mathrm{DD})} = 1/2$, $K_0^{(\mathrm{DD})} = 0$, which closes the first two channels, and $K_1^{(\mathrm{DD})}/\omega^{(\mathrm{DD})} = 2.4048$ which reduces the hopping rate in the third channel to zero. Whereas in the tunneling direction, the directed migration is achieved through our previous modulation scheme of periodically altering $K_1^{(\mathrm{TD})}$ to K_1^A and K_1^B.

In Figure 2, we demonstrate the pair migration along the anticipated route. The results are from the numerical evolution for a 8×8 lattice system. The parameters in the damping directions have been set as described above with $\omega^{(\mathrm{DD})} = \omega^{(\mathrm{TD})} = 40$ (in units of J). In the other direction, we have properly arranged the tunneling scheme proposed in the Section 3. When the correlated pair reaches a particular site, exchanging the conditions for each individual directions can lead to the further migration in the other direction. In Figure 2a, we plotted the density peaks in a 3D histogram at times $t_n = n \cdot (T_A + T_B)$, $n = 0, 1, 2, \cdots$, with n labeled by the color bar. The density evolution along the route is shown in Figure 2b. The density evolves to a maximum value at t_n located at one of the sites, which is consistent with Figure 2a.

5 Generating entanglement

The driving scheme with tilted lattice highly localize a single isolated particle in the 1D space. We can make use of this to realize a interacting process between a single particle and a particle pair. As shown in Figure 3a, two single particles locate at site 3 and site 8, whereas a pair of particles is placed between them. The corresponding modulation shown in Figure 1b leads to the migration of the particle pair. The hopping of the isolated particles can only occur with the assistance of other particles. When the state $|1\rangle_8 \otimes |102\rangle_{3,4,5}$ is formed at time $t = T_A + T_B$, we set $K_1 = K_1^B$ to suppress

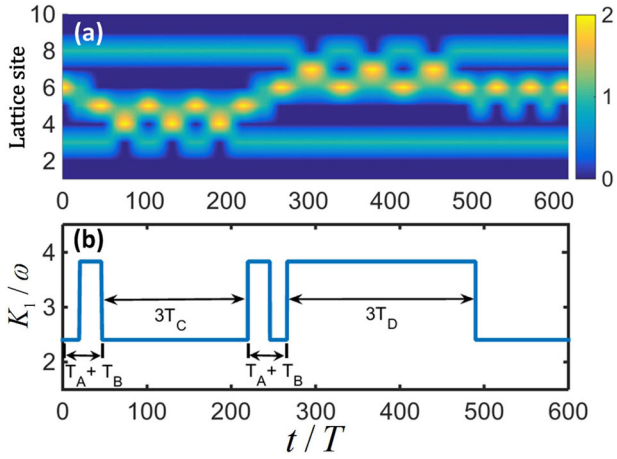

Fig. 3. 4-particle modulation scheme. (a) The density evolutions revealing the migrating, tripartite oscillating and separating processes. After time $t = T_A + T_B + 3T_C + 3T_D$, the pair undergoes the oscillation $|0,2\rangle_{\langle 5,6\rangle} \leftrightarrow |1,1\rangle_{\langle 5,6\rangle}$. (b) The corresponding modulations of the shaking amplitude between the values $K_1^A/\omega = 3.8317$ and $K_1^B/\omega = 2.4048$.

all tunneling processes except

$$|102\rangle_{\langle i,j,k\rangle} \leftrightarrow |111\rangle_{\langle i,j,k\rangle} \leftrightarrow |021\rangle_{\langle i,j,k\rangle}, \tag{6}$$

with the same hopping rate $\tilde{J} = J\mathcal{J}_1(K_1^B/\omega)$. The state $|n_i, n_j, n_k\rangle$ represents the one with n_i, n_j, n_k particles on site i, j, k, respectively, and $\langle i,j,k\rangle$ indicate three neighboring sites *i,j,k*. Since the particle on site 8 remains unaffected, we concentrate on the lower tripartite system which can be described by

$$|\Phi(t)\rangle = c_1(t)|102\rangle_{\langle i,j,k\rangle} + c_2(t)|111\rangle_{\langle i,j,k\rangle} + c_3(t)|021\rangle_{\langle i,j,k\rangle}. \tag{7}$$

By setting $c_1(t=0) = 1$, we have the analytical results

$$\begin{aligned} c_1(t) &= \frac{1}{2}\cos(2\tilde{J}t) + \frac{1}{2}, \\ c_2(t) &= -\frac{i}{\sqrt{2}}\sin(2\tilde{J}t), \\ c_3(t) &= \frac{1}{2}\cos(2\tilde{J}t) - \frac{1}{2}, \end{aligned} \tag{8}$$

with the oscillation periods $T_C = \pi/\tilde{J}$ for both $|c_1(t)|^2$ and $|c_3(t)|^2$ and $T_C/2$ for $|c_2(t)|^2$. The initial state $|102\rangle_{\langle 4,5,6\rangle}$ recovers at time $t = T_A + T_B + nT_C$ ($n = 3$ in our case). Then a $T_A - T_B$ mode modulation separates the three particles into a pair and an isolated one. When the pair interact with the upper particle, the shaking amplitude is set to $K_1 = K_1^A$. Equation (8) also applies with altering the hopping rate to $\tilde{J} = J\mathcal{J}_0(K_1^A/\omega)$ and the oscillation period to $T_D = \pi/\tilde{J}$. After time $t = 2T_A + 2T_B + nT_C + mT_D$ ($n = m = 3$), $K_1 = K_B$ is remained to separate four particles into two isolated particles and an oscillating particle pair.

However, the subtle states remains unclear if we consider distinguishable particles. By studying the internal details, we may be able to realize quantum entanglement within the lattice system. Now we assume the two isolated particles shown in Figure 3a to be *a*-type atoms, whereas the particles in migrating pair, initially located at site 6,

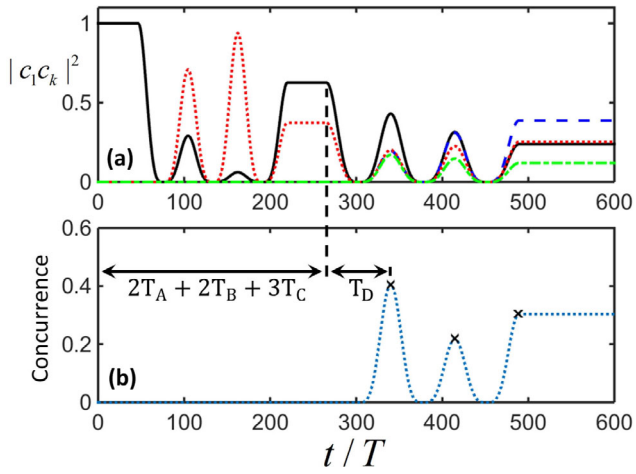

Fig. 4. (a) The probabilities of the internal states with $|c_1c_{00}|^2$ indicated by the black real curve, $|c_1c_{01}|^2$ by the blue dashed curve, $|c_1c_{10}|^2$ by the red dotted curve and $|c_1c_{11}|^2$ by the green dash-dotted curve. The summation of the four quantities gives the possibility of the state $|102\rangle_{\langle i,j,k\rangle}$. (b) The bipartite concurrence calculated from (a). The valid nonzero values of the concurrence are labeled by crosses at times $t = 2T_A + 2T_B + 3T_C + mT_D$ (m = 1,2,3).

are b-type atoms. a,b atoms are distinguishable particles such as neutron bosons of different hyperfine states. We focus on the system composed of two localized particles on site 3 and site 8, which are labeled by system I and system II, respectively. Thus $|\Phi\rangle \in \mathcal{H}_{\rm I} \otimes \mathcal{H}_{\rm II}$, where $\mathcal{H}_{\rm I} = \{|a\rangle \equiv |0\rangle, |b\rangle \equiv |1\rangle\}_{\rm I}$, $\mathcal{H}_{\rm I} = \{|a\rangle \equiv |0\rangle, |b\rangle \equiv |1\rangle\}_{\rm II}$. Such definitions are suitable only when the three parts (two isolated particles and the pair) separate. A two-partite system with two internal states can be decomposed by $|\Phi\rangle = \sum_{i,j=0,1} c_{i,j}|i\rangle_{\rm I} \otimes |j\rangle_{\rm II}$, and the degree of entanglement for such system is generally measured by the concurrence [52]

$$C(\Phi) = 2|c_{00}c_{11} - c_{01}c_{10}|. \tag{9}$$

$C = 1$ indicate a maximal entanglement, such as for the two-qubit Bell states. Whereas $C = 0$ means the two-partite wave function can be factorized.

In our case for the systems I and II, the values of concurrence are valid at time $t = 2T_A + 2T_B + nT_C + mT_D$ (with n,m integers), i.e., when $c_1(t)$ in equation (7) equals one. The concurrence with site-resolved two parts I and II depends on discrete n and m. A simulation has been carried out to show the evolutions of the concurrence. In Figure 4a, we show the probabilities of the internal states: $|c_1c_{00}|^2$ (the black real curve), $|c_1c_{01}|^2$ (the blue dashed curve), $|c_1c_{10}|^2$ (the red dotted curve), $|c_1c_{11}|^2$ (the green dash-dotted curve). The concurrence multiplied by $|c1|^2$ is shown in Figure 4b, where three possible values of $C(\Phi)$ are marked by crosses. Before time $t = 2T_A + 2T_B + 3T_C$, the migrating pair only interact with system I, resulting in nonzero c_{00} and c_{10}, whereas $c_{01} = c_{11} = 0$ and thus $C(\Phi) = 0$. When the oscillation between the pair and system II occurs, c_{01}, c_{11} and $C(\Phi)$ rises. Nonzero concurrence indicate the entanglement of the system I and II, which is produced through successively interacting with the migrating pair.

Since the entanglement is built at the end of the interacting oscillation and subsequent modulations can then be carried out, we arrive at a quantum gate controlled by the modulations of optical lattice. Further applications including parallel processing and higher dimensional operation in this model are available.

6 Summary

In summary, we have investigated correlated atoms in a fast driving Hubbard model. We focus on two cases: the tilted shaking lattice and the DM in a uniform lattice. Both cases can break the mirror symmetry of tunneling, which is the key to realize directed migration of a correlated particle pair. Taking the latter case as an example and in conditions $U_0 = K_0 = \omega/2 \gg J$, we have shown the specific scheme to achieve the migration in 1D and 2D with utilizing the CDTs and the photon-assisted tunneling effects. Further manipulation with isolated particles and the migrating pair were proposed to generate two-partite entanglement.

References

1. I. Bloch, W. Zwerger, Rev. Mod. Phys. **80**, 885 (2008)
2. I. Bloch, J. Dalibard, S. Nascimbne, Nat. Phys. **8**, 267 (2012)
3. W.S. Bakr, J.I. Gillen, A. Peng, S. Fölling, M. Greiner, Nature **462**, 74 (2009)
4. J.F. Sherson, C. Weitenberg, M. Endres, M. Cheneau, I. Bloch, S. Kuhr, Nature **467**, 68 (2010)
5. M.F. Parsons, F. Huber, A. Mazurenko, C.S. Chiu, W. Setiawan, K. Wooley-Brown, S. Blatt, M. Greiner, Phys. Rev. Lett. **114**, 213002 (2015)
6. D. Jaksch, C. Bruder, J.I. Cirac, C.W. Gardiner, P. Zoller, Phys. Rev. Lett. **81**, 3108 (1998)
7. M. Greiner, O. Mandel, T. Esslinger, T.W. Hänsch, I. Bloch, Nature **415**, 39 (2002)
8. R. Jôrdens, N. Strohmaier, K. Günter, H. Moritz, T. Esslinger, Nature **455**, 204 (2008)
9. S. Murmann, A. Bergschneider, V.M. Klinkhamer, G. Zurn, T. Lompe, S. Jochim, Phys. Rev. Lett. **114**, 080402 (2015)
10. M. Aidelsburger, M. Atala, M. Lohse, J.T. Barreiro, B. Paredes, I. Bloch, Phys. Rev. Lett. **111**, 185301 (2013)
11. H. Miyake, G.A. Siviloglou, C.J. Kennedy, W.C. Burton, W. Ketterle, Phys. Rev. Lett. **111**, 185302 (2013)
12. R.N. Palmer, A. Klein, D. Jaksch, Phys. Rev. A **78**, 013609 (2008)
13. A.S. Sørensen, E. Demler, M.D. Lukin, Phys. Rev. Lett. **94** (2005)
14. R.N. Palmer, D. Jaksch, Phys. Rev. Lett. **96**, 180407 (2006)
15. M. Hafezi, A.S. Sørensen, E. Demler, M.D. Lukin, Phys. Rev. A **76** (2007)
16. A. Polkovnikov, K. Sengupta, A. Silva, M. Vengalatore, Rev. Phys. **93**, 863 (2011)
17. J. Eisert, M. Friesdorf, C. Gogolin, Nat. Phys. **11**, 124 (2015)
18. M. Holthaus, D.W. Hone, Phil. Mag. Part B **74**, 105 (1996)
19. N. Goldman, J. Dalibard, Phys. Rev. X **4**, 031027 (2014)
20. C. Sias, H. Lignier, Y.P. Singh, A. Zenesini, D. Ciampini, O. Morsch, E. Arimondo, Phys. Rev. Lett. **100**, 040404 (2008)
21. D.H. Dunlap, V.M. Kenkre, Phys. Rev. B **34**, 3625 (1986)
22. S. Longhi, J. Phys. Condens. Matter. **24**, 435601 (2012)
23. F. Grossmann, T. Dittrich, P. Jung, P. Hanggi, Phys. Rev. Lett. **67**, 516 (1991)
24. J.M. Villas-Bôas, S.E. Ulloa, N. Studart, Phys. Rev. B **70**, 041302 (2004)
25. H. Lignier, C. Sias, D. Ciampini, Y. Singh, A. Zenesini, O. Morsch, E. Arimondo, Phys. Rev. Lett. **99**, 220403 (2007)
26. J. Gong, L. Morales-Molina, P. Hänggi, Phys. Rev. Lett. **103**, 133002 (2009)
27. S. Longhi, Phys. Rev. A **86**, 044102 (2012)
28. K. Hai, W. Hai, Q. Chen, Phys. Rev. A **82**, 053412 (2010)
29. S. Longhi, G. Della Valle, Phys. Rev. A **86**, 043633 (2012)
30. G. Lu, L.-B. Fu, J. Liu, W. Hai, Phys. Rev. A **89**, 033428 (2014)
31. F. Meinert, M.J. Mark, K. Lauber, A.J. Daley, H.-C. Nagerl, Phys. Rev. Lett. **116**, 205310 (2016)
32. T.E. Lee, Phys. Rev. A **94**, 040701(R) (2016)

33. C.E. Creffield, Phys. Rev. Lett. **99**, 110501 (2007)
34. W.S. Dias, M.L. Lyra, F.A.B.F. de Moura, Phys. Lett. A **374**, 44 (2010)
35. D. Souza, F. Claro, Phys. Rev. B **82**, 205437 (2010)
36. R. Khomeriki, D.O. Krimer, M. Haque, S. Flach, Phys. Rev. A **81**, 065601 (2010)
37. S. Longhi, Phys. Rev. B **86**, 043633 (2012)
38. Y. Zheng, S.-J. Yang, New J. Phys. **18**, 013005 (2015)
39. Y. Zheng, S.-J. Yang, Phys. Rev. A **93**, 063609 (2016)
40. S. Greschner, L. Santos, D. Poletti, Phys. Rev. Lett. **113**, 183002 (2014)
41. Á. Rapp, X. Deng, L. Santos, Phys. Rev. Lett. **109**, 203005 (2012)
42. M. Diliberto, C.E. Creffield, G.I. Japaridze, C.M. Smith, Phys. Rev. A **89**, 013624 (2014)
43. A. Eckardt, C. Weiss, M. Holthaus, Phys. Rev. Lett. **95**, 260404 (2005)
44. A. Eckardt, M. Holthaus, Europhys. Lett. **80**, 50004 (2007)
45. P.M. Preiss, R. Ma, M.E. Tai, A. Lukin, M. Rispoli, P. Zupancic, Y. Lahini, R. Islam, M. Greiner, Science **347**, 1229 (2015)
46. Y. Kaluzny, P. Goy, M. Gross, J.M. Raimond, S. Haroche, Phys. Rev. Lett. **51**, 1175 (1983)
47. S. Fölling, S. Trotzky, P. Cheinet, M. Feld, R. Saers, A. Widera, T. Muller, I. Bloch, Nature (London) **448**, 1029 (2007)
48. A. Eckardt, M. Holthaus, H. Lignier, A. Zenesini, D. Ciampini, O. Morsch, E. Arimondo, Phys. Rev. A **79**, 013611 (2009)
49. W.S. Bakr, A. Peng, M.E. Tai, R. Ma, J. Simon, J.I. Gillen, S. Foelling, L. Pollet, M. Greiner, Science **329**, 547 (2010)
50. J.W. Britton, B.C. Sawyer, A.C. Keith, C.-C.J. Wang, J.K. Freericks, H. Uys, M.J. Biercuk, J.J. Bollinger, Nature **484**, 489 (2012)
51. A. Schreiber, A. Gbris, P.P. Rohde, K. Laiho, M. Štefaňák, V. Potoček, C. Hamilton, I. Jex, C. Silberhorn, Science **336**, 55 (2012)
52. R. Lohmayer, A. Osterloh, J. Siewert, A. Uhlmann, Phys. Rev. Lett. **97**, 260502 (2006)